



Short communication

## Preparation of Li–Mn–O thin films by r.f.-sputtering method and its application to rechargeable batteries

S. KOMABA<sup>1</sup>, N. KUMAGAI<sup>1</sup>, M. BABA<sup>1</sup>, F. MIURA<sup>1</sup>, N. FUJITA<sup>1</sup>, H. GROULT<sup>2</sup>,  
D. DEVILLIERS<sup>2</sup> and B. KAPLAN<sup>2</sup>

<sup>1</sup>Faculty of Engineering, Iwate University, Morioka 020-8551, Japan

<sup>2</sup>Pierre & Marie Curie University, 4, Place Jussieu-Batiment, F 75252, Paris Cedex 05, France

Received 2 February 2000; accepted in revised form 2 May 2000

**Key words:** LiMn<sub>2</sub>O<sub>4</sub>, lithium battery, lithium intercalation, r.f.-sputtering, thin film

### Abstract

Spinel-LiMn<sub>2</sub>O<sub>4</sub> thin films were fabricated on stainless steel substrate by the r.f.-sputtering method. They were annealed within the range 400–700 °C for 1 h in O<sub>2</sub> and their electrochemical performance was compared to that of as-deposited film. The thin films were characterized by X-ray diffractometry and electron spectroscopy for chemical analysis (ESCA). Charge–discharge tests were carried out in an LiClO<sub>4</sub>/propylene carbonate solution. The films heat-treated at 400–700 °C exhibited excellent cyclability over a wide potential region from 2.0 to 4.3 V vs Li/Li<sup>+</sup>.

### 1. Introduction

Recently, much attention has been devoted to lithium rechargeable batteries, due to the development of miniaturized electronic devices such as cellular phones, camcorders and notebook computers. Although LiCoO<sub>2</sub> has been used as the cathode for commercial lithium ion batteries from 1991, the cost of the raw materials is relatively high and the estimated amount of cobalt materials in the earth is limited. Hence, other oxides are under active research. Manganese based oxides are one of most promising candidates as cathode material because they possess a high theoretical energy density and can be synthesized from low cost and lower toxicity materials [1].

If thin films of the active materials can be applied to lithium rechargeable batteries, they will realize a thin film power source with high energy density, which is able to be adopted as a memory back up battery in small IC cards. In recent years, several thin film electrodes, such as TiS<sub>2</sub> [2], V<sub>2</sub>O<sub>5</sub> [3] and LiMn<sub>2</sub>O<sub>4</sub> [4, 5], have been researched for microbattery application. As described by Shokoochi et al. [4], LiMn<sub>2</sub>O<sub>4</sub> thin films prepared by electron-beam evaporation showed good cyclability, that is 70% of initial capacity was sustained after 220 cycles. Hwang et al. [5] researched LiMn<sub>2</sub>O<sub>4</sub> thin films formed by r.f.-magnetron sputtering which showed good cyclability with almost no capacity loss after ≥1000 cycles utilizing a 4 V plateau. As reported by Wang et al. [6], LiCoO<sub>2</sub> thin films fabricated by the r.f.-magnetron sputtering method hardly showed capacity fading after 10000 cycles. Furthermore, an all-solid-state

microbattery, which can be applied for memory back up, was described by Jones et al. [7], and solid state microbatteries of TiS<sub>2</sub>, V<sub>2</sub>O<sub>5</sub> or LiMn<sub>2</sub>O<sub>4</sub>/Lipon/Li were reported by Bates and coworkers [8]. We also described the battery performance of Nb<sub>2</sub>O<sub>5</sub> and V<sub>2</sub>O<sub>5</sub> thin films formed by r.f.-sputtering [9, 10]. Very recently, we reported that a V<sub>2</sub>O<sub>5</sub>/Lipon/Li<sub>x</sub>V<sub>2</sub>O<sub>5</sub> solid-state battery demonstrated excellent cyclability [11]. In this work, we prepared spinel LiMn<sub>2</sub>O<sub>4</sub> thin films by r.f.-sputtering and investigated the cyclability over the wider potential region of 2.0–4.3 V.

### 2. Experimental details

Thin films were deposited by r.f.-sputtering of a pure LiMn<sub>2</sub>O<sub>4</sub> target (Kojundo Kagaku Co., purity ≥99%, 78 mm dia. × 3 mm) on stainless steel substrates (SUS 304, thickness 0.03 mm). The r.f.-power was 100 W and the Ar pressure was 80 mtorr. Films had an area of 1 × 1 cm<sup>2</sup>, and the deposition period was 240 min. After the deposition by r.f.-sputtering, the thin films deposited were annealed in an O<sub>2</sub> atmosphere. The characterization of the films was carried out by X-ray diffractometry (XRD) using Cu K<sub>α</sub> radiation and electron spectroscopy for chemical analysis (ESCA) using Al K<sub>α</sub> radiation. The film thickness was measured with multiple beam interferometry (MIB).

Electrochemical measurements were carried out in a three-electrode beaker type cell at 25 ± 2 °C. Reference and counter electrodes used were lithium metal, and the thin films were used as a working electrode. The

electrolyte solution used was 1 M  $\text{LiClO}_4$ -propylene carbonate (PC). Cells were assembled inside an Ar atmosphere glove box. Charge–discharge measurements were carried out in the range 2.0–4.3 V vs  $\text{Li/Li}^+$  at  $0.01 \text{ mA cm}^{-2}$ .

### 3. Results and discussion

The SEM photograph of the Li–Mn–O thin film on the flat silicon substrate is shown in Figure 1. The morphology of the film is very uniform and thickness is in the range 0.3–0.5  $\mu\text{m}$ .

Figure 2 shows X-ray diffraction patterns of the films deposited on a stainless steel substrate before and after heat treatment at various temperatures for 1 h. In the case of the as-deposited thin film, the crystallinity is very low because of the clear appearance of only a substrate peak. When the temperature was increased to 750  $^\circ\text{C}$ , a characteristic peak around  $2\theta = 18.6^\circ$ , corresponding to spinel- $\text{LiMn}_2\text{O}_4$  (111) diffraction, appears and gradually becomes sharper and stronger. Hence, the crystallinity of the films gradually increased with increasing the heat treatment temperature. We confirmed that a similar result was obtained when a shorter period of heat treatment of 5 min was used. Hence, we consider that the crystallization and oxidation of the films are completed by heat treatment within 1 h in  $\text{O}_2$  atmosphere.

The initial discharge behaviors of the as-deposited and heat treated films for 1 h are shown in Figure 3. Although the thickness of all samples was in the same range of 0.3–0.5  $\mu\text{m}$ , an accurate determination of the film thickness, that is, amount of the active material, was difficult by MIB because of the roughness of the stainless steel substrate. Hence, we characterized the oxide films by comparing the discharge periods obtained at the same current density. The as-deposited film hardly shows a potential plateau around 4 V, originating from the spinel-related structure, that is, it agrees with the

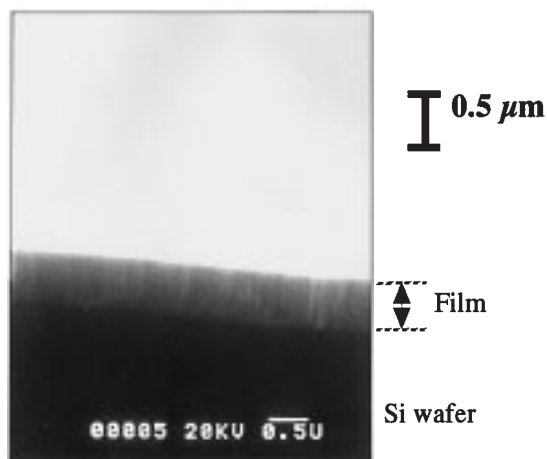


Fig. 1. Cross sectional image of an as-deposited lithium manganese oxide thin film formed on Si wafer by r.f.-sputtering method.

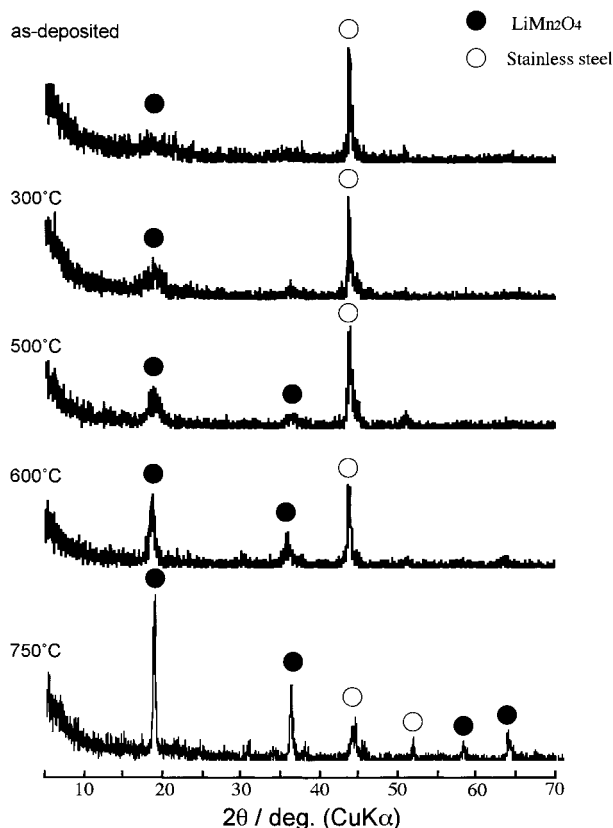


Fig. 2. X-ray diffraction patterns of lithium manganese oxide thin films on stainless steel heat-treated at various temperatures for 1 h in  $\text{O}_2$ .

XRD result. On the other hand, the heat-treated samples shows two potential plateaus around 4 V and 3 V, which are typically observed for spinel- $\text{LiMn}_2\text{O}_4$  [12]. Although the crystallinity was increased by increasing the heat treatment temperature up to 750  $^\circ\text{C}$ , the sample treated at 500  $^\circ\text{C}$  exhibited the highest capacity with a similar curve to the typical spinel- $\text{LiMn}_2\text{O}_4$ . Generally, the synthesis of  $\text{LiMn}_2\text{O}_4$  powder was carried out at the optimum temperature of 750  $^\circ\text{C}$  [13]. Heat treatment within 600–700  $^\circ\text{C}$  drastically decreased the discharge capacity.

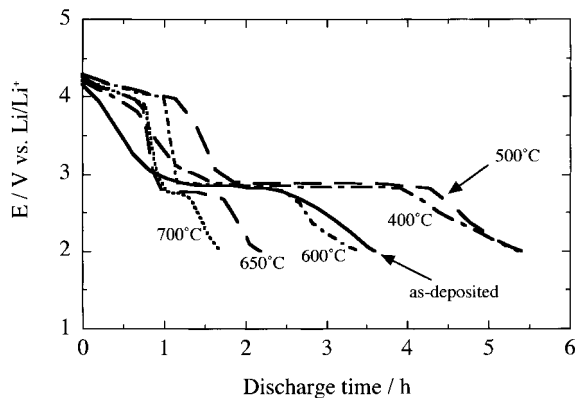


Fig. 3. Initial discharge curves of lithium manganese oxide thin films heat-treated at various temperatures for 1 h in  $\text{O}_2$  and an as-deposited thin film.

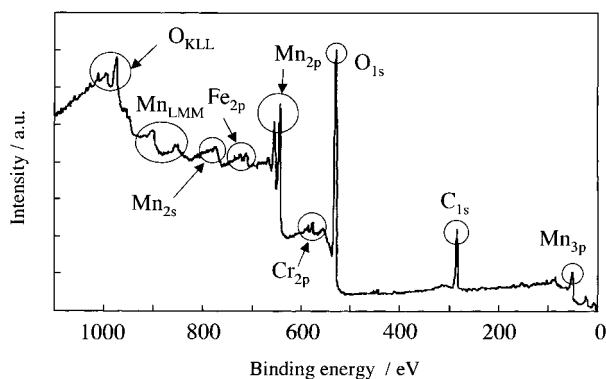


Fig. 4. XPS spectra of a lithium manganese oxide thin film heat-treated at 650 °C for 1 h.

To clarify the effect of the higher temperature heat treatment, elemental analysis of the thin film was performed with ESCA. An ESCA spectrum of the thin film treated at 650 °C is shown in Figure 4. Clearly, Mn(2p) and O(1s) peaks appear in the spectrum. Moreover, small peaks of Fe(2p) and Cr(2p) are also observed. It is likely that C(1s) peak at 287 eV is due to contamination of organic impurities from air. They confirm the existence of Mn, O, Fe, and Cr at the surface of the film. Figure 5 shows depth profiles of the chemical composition estimated from the ESCA spectra with sputtering of the thin film. It is clear that definite amounts of Fe and Cr existed in the whole film. We

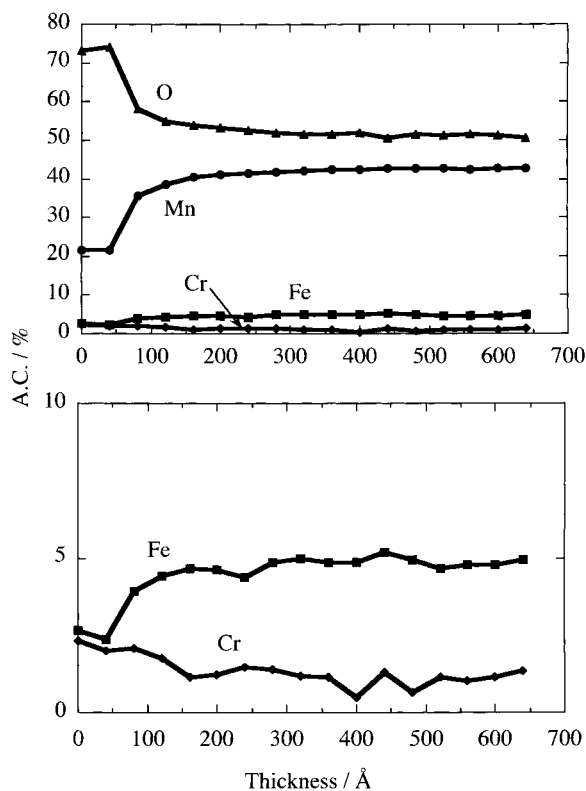


Fig. 5. Depth profile of compositions of a thin film heat-treated at 650 °C for 1 h estimated from XPS spectra.

believe that the appearance of iron and chromium was due to the thermal diffusion from the SUS substrate during heat treatment at 650 °C. It is likely that the thin film consists of a solid solution of  $\text{Li}(\text{Cr}, \text{Fe})_x\text{Mn}_{2-x}\text{O}_4$ , that is, the 16d site of manganese is partially substituted with Cr and Fe. As reported previously, these partial substitutions with Cr [13, 14] and Fe [15, 16] in the 16d site are expected to enhance the overall structural stability because of the suppression of Jahn–Teller distortion caused by  $\text{Mn}^{3+}$  ( $t_{2g}^3 e_g^1$ ).

As described in Figure 3, the initial discharge capacity was decreased by increasing the heat treatment temperature from 500 to 700 °C, though the crystallinity was enhanced at higher temperature. In consideration of the XRD, discharge capacity and ESCA results, the heat treatment resulted in the enhancement of crystallinity and the formation of  $\text{Li}(\text{Cr}, \text{Fe})_x\text{Mn}_{2-x}\text{O}_4$ . Thus, the treatment at about 500 °C is effective for high capacity owing to both of the higher crystallinity and the appropriate amount of the substitution elements.

Figure 6 shows charge–discharge cycling behavior for the oxide films before and after heat treatment at 600 °C for 1 h. Using the average film thickness (0.4  $\mu\text{m}$ ) and the density of  $\text{LiMn}_2\text{O}_4$  (4.281  $\text{g cm}^{-3}$ ), the discharge capacity corresponding to the period of 3.5 h was roughly estimated to be  $>200 \text{ mAh (g-oxide)}^{-1}$  from 4.3 to 2.0 V. The as-deposited sample indicated that charge–discharge capacity considerably decreased with increasing cycle number. The capacity at the 20th cycle

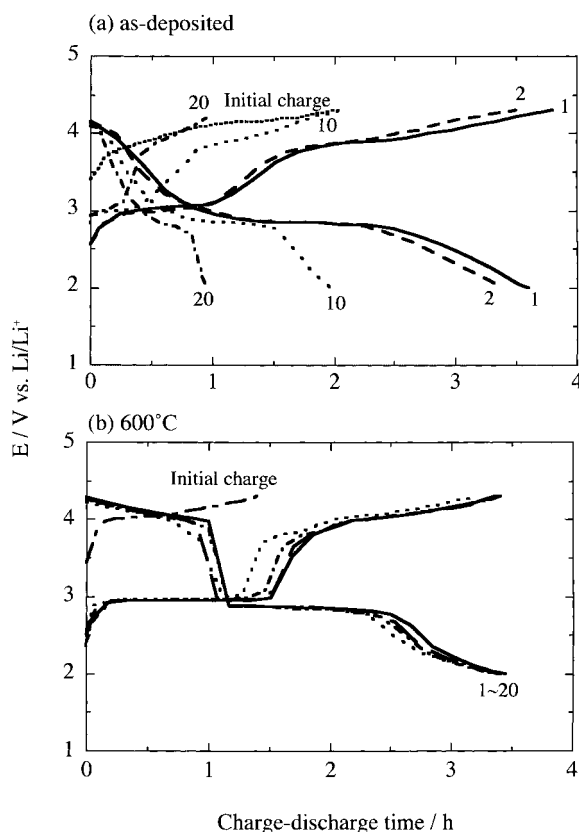


Fig. 6. Charge–discharge curves of (a) an as-deposited thin film and (b) a thin film heat-treated at 600 °C for 1 h.

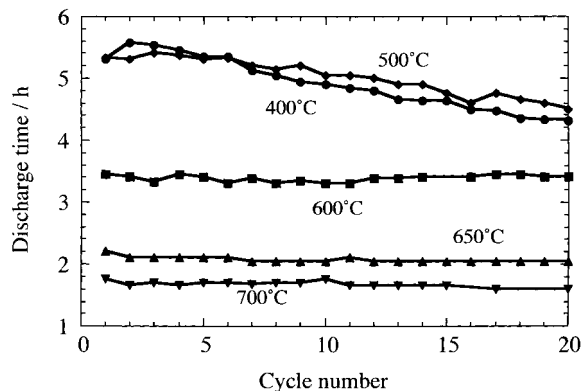


Fig. 7. Cycle number against discharge time plots of thin films heat-treated at various temperatures for 1 h in  $O_2$ .

was reduced to about one fourth of the initial value. The capacity loss seemed to be due to the amorphous nature of the film and, furthermore, the thin film peeled off the substrate during charge–discharge cycling.

On the other hand, as shown in Figure 6(b), another sample annealed at 600 °C demonstrated excellent cyclability in spite of the wide potential region between 4.3 and 2.0 V. As clearly shown in Figure 6(b), typical plateaux at 4 V and 3 V appear and hardly change over 20 cycles. Generally, in the case of the  $LiMn_2O_4$  powder sample, the cycling behaviour in the wider range from 4.0 to 2.0 V is poor [15] because of the large volume change of about 5.6% during lithium insertion in the 3.0 V plateau region [12]. This difference is likely due to the geometry of the film which is markedly different from  $LiMn_2O_4$  powder. On the other hand, Jang et al. reported that spinel Li–Mn–O, obtained through electrochemical cycling of orthorhombic  $LiMnO_2$ , showed excellent cyclability when both the 4.0 V and 3.0 V intercalation plateaux were utilized [17]. This spinel phase contained partial tetrahedral cation site occupancy and nanodomain structure (20–50 nm size). Jang et al. suggested that this structure was responsible for the cycling stability of the electrochemically produced spinel. It is likely that the heat treated film also possesses similar micro structure and/or higher plasticity. Further analysis is needed to confirm this structure.

As shown in Figure 7, the variation in discharge capacity during the initial 20 cycles was compared among the samples treated at various temperatures. The cycling behaviors are dependent on the temperature, and hardly dependent on the thickness. Samples annealed at 400 °C and 500 °C have higher capacity, but show faster capacity fade, compared to samples annealed at more than 600 °C. We investigated the extended cycling

behaviour of the film heat treated at 650 °C for 1 h and obtained excellent cyclability over more than 100 cyclings.

From these results we conclude that the spinel Li–Mn–O thin film formed by r.f.-sputtering exhibited stable cycling performance in the wide potential region 4.3–2.0 V vs  $Li/Li^+$  in organic electrolyte solution. In future studies we will report the application of this Li–Mn–O film to solid state film type microbatteries.

### Acknowledgements

This work was financially supported by a grant-in-aid for International Scientific Research: University-to-University Cooperative Research, by the Japanese Ministry of Education, Science, and Culture, The Iwatani Naoji Foundation's Research Grant, and Yazaki Memorial Foundation for Science & Technology.

### References

1. J.M. Tarascon and D. Guyomard, *Electrochim. Acta.* **38** (1993) 1221.
2. Z. Takehara, Z. Ogumi, Y. Uchimoto, E. Endo and Y. Kanamori, *J. Electrochem. Soc.* **138** (1991) 1574.
3. K. West, B. Zachau-Christiansen, S.V. Skaarup and F.W. Poulsen, *Solid State Ionics* **57** (1992) 41.
4. F.K. Shokoohi, J.M. Tarascon, B.J. Wilkens, D. Guyomard and C.C. Chang, *J. Electrochem. Soc.* **139** (1992) 1845.
5. K.-H. Hwang, S.-H. Lee and S.-K. Joo, *J. Electrochem. Soc.* **141** (1994) 3296.
6. B. Wang, J.B. Bates, F.X. Hart, B.C. Sales, R.A. Zuhr and J.D. Robertson, *J. Electrochem. Soc.* **143** (1996) 3203.
7. Steven D. Jones and James R. Akridge, *Solid State Ionics* **53–56** (1992) 628.
8. J.B. Bates, G.R. Gruzalski, N.J. Dudney, C.F. Luck and Xiaohua Yu, *Solid State Ionics* **70–71** (1994) 619.
9. N. Kumagai, Y. Tateshita, Y. Takatsuka, M. Baba, T. Ikeda and K. Tanno, *J. Power. Sources.* **54** (1995) 175.
10. N. Kumagai, H. Kitamoto, M. Baba, S. Durand-Vidal, D. Devilliers and H. Groult, *J. Appl. Electrochem.* **28** (1998) 41.
11. M. Baba, N. Kumagai, H. Kobayashi, O. Nakano and K. Nishidate, *Electrochem. & Solid State Lett.* **2**(7) (1999) 320.
12. T. Ohzuku, M. Kitagawa and T. Hirai, *J. Electrochem. Soc.* **137** (1990) 769.
13. Li Guohua, H. Ikuta, T. Uchida and M. Wakihara, *J. Electrochem. Soc.* **143** (1996) 178.
14. M. Hosoya, H. Ikuta and M. Wakihara, *Solid State Ionics* **111** (1998) 153–9.
15. J.M. Tarascon, E. Wang, F.K. Shokoohi, W.R. Mckinnon and S. Colson, *J. Electrochem. Soc.* **138** (1991) 2859.
16. M.Y. Song, D.S. Ahn, S.G. Kang and S.H. Chang, *Solid State Ionics* **111** (1998) 237–42.
17. Y.I. Jang, B. Huang, H. Wang, D.R. Sadoway and Y.-M. Chiang, *J. Electrochem. Soc.* **146** (1999) 3217–23.